



Effect of activating fluxes on the geometry, hardness, and microstructure of 316L stainless steel in GMAW

Huifeng Wang¹ · Stefanija Klaric¹

Received: 18 March 2024 / Accepted: 1 September 2024

© The Author(s), under exclusive licence to Springer-Verlag London Ltd., part of Springer Nature 2024

Abstract

Activating fluxes (AF) can be applied in the welding process to improve the morphology, microstructure, and mechanical properties, such as hardness, tensile strength, and yield strength. Regarding the published research on AF application in Tungsten Inert Gas (TIG) welding, there are limited studies concerning the Gas Metal Arc Welding (GMAW) process. This gap in research has prompted investigations aimed at determining the influence of AF during the GMAW process. The purpose of this paper is to apply three types of AF (SiO_2 , TiO_2 , and CaCO_3) in 316L stainless steel GMAW processing and analyze their influence on the weld bead geometry, hardness, and microstructure. The results showed that the highest penetration and the smallest width can be obtained using TiO_2 as AF while the highest reinforcement can be obtained by CaCO_3 as AF. This also indicated a possible significant increase in AF addition after-welding hardness, which may be caused due to the microstructure changes. The microstructure observation revealed that the welding area without AF was mainly composed of austenite and the addition of AF increased the welding temperature, which caused the martensite structure to be found in these samples. The heat treatment was introduced to reduce the hardness since large and uneven hardness would bring negative consequences such as brittleness. The after-HT analysis showed that HT can reduce the hardness effectively and improve the uniformity of the whole weld bead. Additionally, it was found that samples with AF were more sensitive to HT. This study concludes that AF can be applied in the GMAW welding process and influence the weld bead significantly.

Keywords Gas Metal Arc Welding (GMAW) · Activating fluxes (AF) · Hardness · Microstructure · Heat treatment (HT)

1 Introduction

Activating flux (AF) is a mixture of inorganic materials suspended in a volatile medium, which can be applied on substrate surfaces by painting or spraying. Applications of activating fluxes can improve weld penetration and the mechanical properties of the weld bead. They are effective in joining various compounds such as stainless steel, mild steel, nickel-based alloys, and magnesium-based alloys [1–4] and can be utilized in multiple welding processes, including tungsten inert gas (TIG) [2, 5–7], Gas Metal Arc Welding (GMAW) [1], and laser welding [8, 9]. Their application is widespread and commonly used to increase penetration, reduce energy input, enhance mechanical properties, and influence the microstructure of the weld bead [10]. The

GMAW process [11] was developed in the last century as a high-efficiency welding technology due to its many advantages such as high production efficiency, low welding costs, wide application range, good welding quality, simple operation, and easy mastering.

However, activating fluxes are primarily used in TIG welding now [12–14], and only a few papers report studies on the application of AF in the GMAW process [2]. From the research of AF in GMAW, there is evidence showing that it would be possible to improve mechanical properties or productivity, as described below.

Chakraborty et al. [15] employed three different AF, $(\text{NH}_4)_2(\text{FeSO}_4)_2$, NaHCO_3 , and $(\text{NH}_4)_2\text{CO}_3$, during the GMAW process for SS-202 welding. It was revealed that the highest depth of penetration was obtained with $(\text{NH}_4)_2(\text{FeSO}_4)_2$ as AF, and the minimum and maximum bead widths were obtained using $(\text{NH}_4)_2(\text{FeSO}_4)_2$ and NaHCO_3 , respectively. Furthermore, the hardness testing data showed that AF can increase the weld hardness.

✉ Huifeng Wang
huifeng.wang@students.cdu.edu.au

¹ Charles Darwin University, Casuarina, Australia

Balázs Varbai et al. [16] applied eight AF during GMAW using ER70S-6 as welding wire and EN 1.0421 grade structural carbon steel as base material. The weld geometry, microstructure, and hardness were studied. The highest face height can be obtained using MnO while $MgCO_3$ helped achieve the highest penetration. However, there were no significant differences in hardness distribution and the microstructure with and without AF.

Chaudhari et al. [4] applied the AHP (Analytic Hierarchy Process)-MOORA (multi-objective optimization based on ratio analysis) and ASRS (Additive Ratio Assessment) method to optimize the GMAW welding process parameters for SS316L. Thus, the results indicated achievement of enhanced penetration in weld was achieved with the use of fluxes SiO_2 , and Cr_2O_3 , and the increase of penetration mechanism with AF.

Huang [2] applied Fe_2O_3 , SiO_2 , and $MgCO_3$ as the AF in AISI 1020 carbon steel GMAW processing. The results revealed that the application of AF in GMAW can increase weld penetration and weld depth/width ratio, reduce the angular distortion, and increase the tensile strength and hardness. It also showed that $MgCO_3$ flux had the most noticeable effect for higher tensile strength.

In the report of Ruan et al. [17], GMAW twin wire with (SiO_2) and without AF was studied for the 6082-T6 Al-alloy plate. Results have shown that the addition of the AF had no significant effects on the microstructure in both joint and HAZ. There was about a 26% increase in penetration depth with AF. It was also revealed that the microhardness and strength of the weld joint were not influenced by SiO_2 .

To increase the mechanical properties, Moorthy et al. [18] applied AF (TiO_2 , Al_2O_3 , and Fe_2O_3) in the GMAW welding processes for mild steel. The study showed that the addition of the AF can increase the tensile strength and TiO_2 can be helpful for higher results compared to the other two AF.

As mentioned above, SiO_2 and TiO_2 were already applied as AF for the GMAW process, and the effects on welding beads geometry and properties were significant, so they were included in this study as well. On the other hand, although there is not as wide application in the research as the above-mentioned two AF, due to its physics characteristics (i.e., it can be decomposed into CaO and CO_2) during the welding process and results reported by [19], $CaCO_3$ was also included in this investigation.

Post-weld heat treatment (PWHT) is a process to improve performances for weld beads, such as the improvement in the mechanical properties, reduction of hardness, and microstructural changes [20]. It will be applied in this study to compare the influence of PWHT on the weld beads produced with and without AF.

The main purpose of his study is to analyze the influence of AF on a single layer (one weld bead), which will be the preliminary research for additive manufacturing since AM

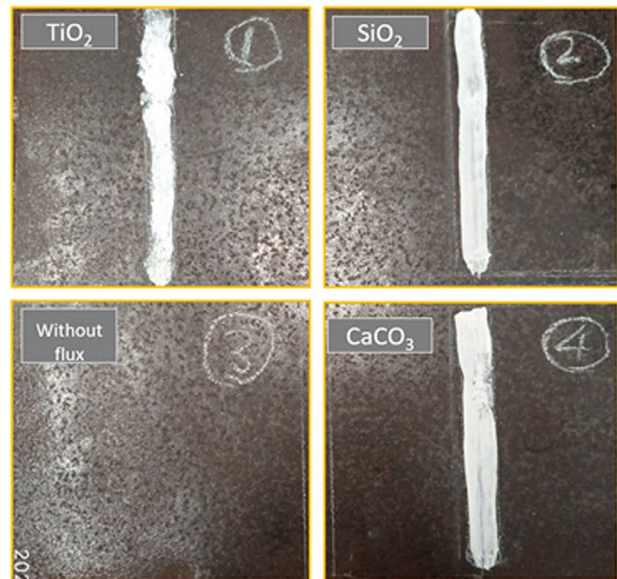


Fig. 1 Activating flux application

Table 1 Welding parameters and experiment design

Welding factors	Value	Experiment design	
Wire feed speed (cm/min)	700	BM	Q235 (5 mm)
Welding speed (cm/min)	36	Wire arc	316L ($\varnothing 1.2$ mm)
Argon feed speed(L/min)	15	AF	SiO_2 , TiO_2 , and $CaCO_3$

is a layer-by-layer accumulation process [21] and the quality of each layer can influence the final quality of the whole product.

2 Experimental procedure

In this section, Q235 mild steel of 5 mm thickness was chosen as the base material (BM), and ER316L stainless steel welding wire was applied as the welding material. The composition of Q235 is C 0.2%, Si 0.35%, Mn 1.4%, P 0.045%, S 0.045%, Cr 0.3%, and Ni 0.3% [22]. The composition of 316L stainless (arc wire ER316L) is C 0.016%, Si 0.51%, Mn 2.14%, P 0.013%, S 0.014%, Cr 18.96%, Cu 0.03%, Ni 12.73%, and Mo 2.32% [23], and the remainder is Fe. Three activating fluxes (SiO_2 , TiO_2 , and $CaCO_3$) are applied with acetone as the solvent. Activating powder was dissolved in the acetone to prepare a paste, and then a brush coat was applied on the surface of the substrate and left to dry before proceeding to the welding, as shown in Fig. 1.

Table 1 shows the welding parameters and the experiment design. During the welding process, Argon was applied as the inert gas with a feed speed of 15 L/min to prepare the



Fig. 2 The FANUC welding robot set-up used in the experiment

bead-on plate (BOP) welds, a travel speed of 36 cm/min and a wire feed speed of 700 cm/min. The FANUC Robot M-10ia with Lincoln S350 power wave was applied as the welding set as shown in Fig. 2.

After welding, four weld beads were obtained, and the appearance of weld beads is shown in Fig. 3. Next, the

welding bead geometry (including the penetrations, reinforcements, and width) of the beads was measured and analyzed.

According to the experimental aim, a microstructural sample preparation is required. In this experiment, the ATM Brilliant 221 cutting machine, mounting machine (Struers CitoPress-1), and automatic polishing machine (Struers TegraPol-15) were used for specimen preparation. The Vickers hardness was tested after the polishing and before etching with a setting of 5 KN load and a 5-s dwell timer using the Struers Durascan hardness tester.

To observe the microstructure, a 4 vol.% nitric acid-alcohol solution was applied for the Base Metal (BM) and Heat Affected Zone (FAZ), while the Kalling No. 2 reagent was used as an etching solution for the weld metal (WM). Figure 4 shows the specimen after etching, which has clear weld boundaries that allow for weld geometry.

After the hardness measurement, the heat treatment (HT) was considered to reduce the hardness of the weld beads and refine the grain size. According to the heat treatment strategy of Kan et al. [24] and Jorge et al. [25], an annealing temperature of 600 °C and 60 min of annealing time with air cooling was applied.

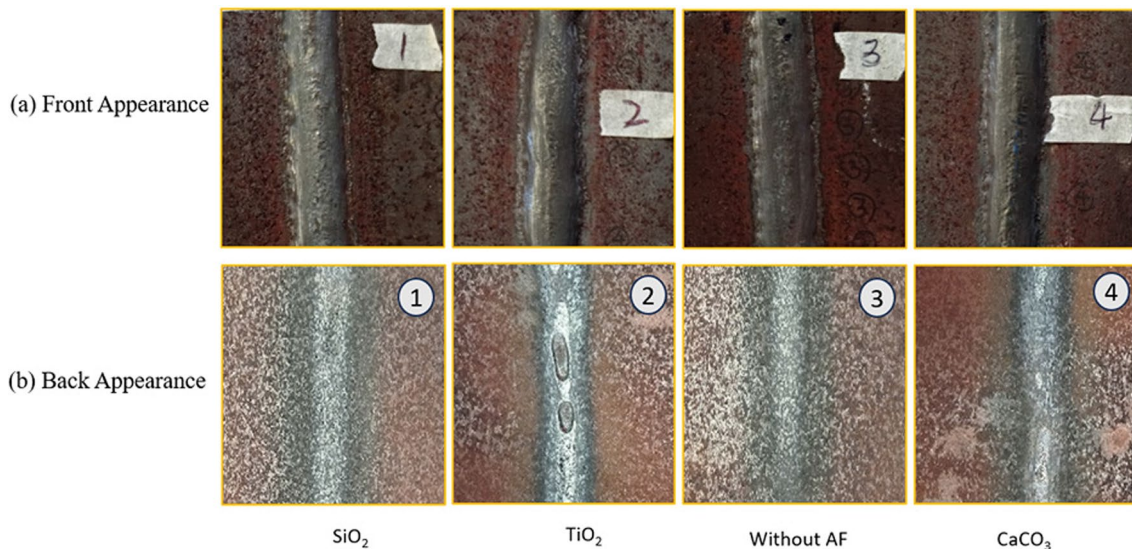


Fig. 3 The appearance of welding beads

Fig. 4 Samples after etching of Kalling No. 2

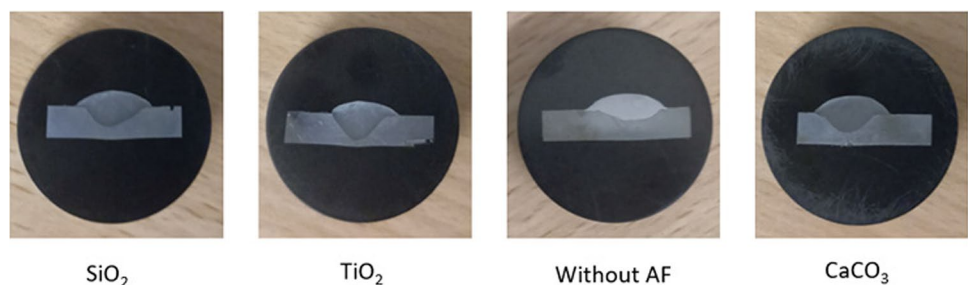


Table 2 Geometry measurement of the weldment

Sample	AF type	Penetration (mm)	Reinforcements (mm)	Width (mm)
1	SiO ₂	2.4	3.16	12.42
2	TiO ₂	3.85	2.95	11.15
3	Without AF	1.5	2.25	13.45
4	CaCO ₃	2.82	3.47	12.16

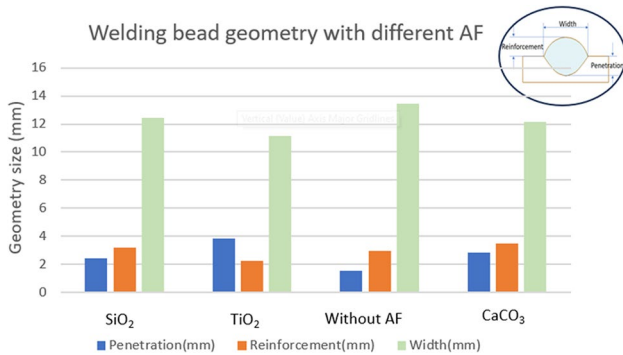


Fig. 5 Variation in bead dimensions with fluxes

3 Results and discussion

3.1 The welding bead geometry

The welding bead appearance is an important indicator of the welding process’s effectiveness, and the geometry can be impacted by different welding parameters. In the procedure presented above, it was observed that all welding beads were able to reach a good appearance without visible splattering. However, they were not uniform enough during the arc closing stage, as shown in Fig. 3a.

It is also indicated that the temperature was not the same during all welding processes, as shown in Fig. 3b. The sample with TiO₂ as the AF, melted through the back metal despite there being no such phenomenon for the other samples. A higher temperature would have allowed a deeper penetration, and it will be illustrated in the following analysis of the variation in bead dimensions.

After etching, a digital vernier caliper was applied to measure the dimensions, which include the average of the bead width, bead height(reinforcement), penetration depth, and aspect ratio (D/W), as shown in Table 2 and Fig. 5.

The penetration, reinforcement, and width of welding beads are considered in this section. As shown in Fig. 5, the highest depth of penetration was obtained using TiO₂ as AF, and the least one was found for the sample without AF. The maximum and minimum bead widths were obtained from the samples without AF and TiO₂ as AF

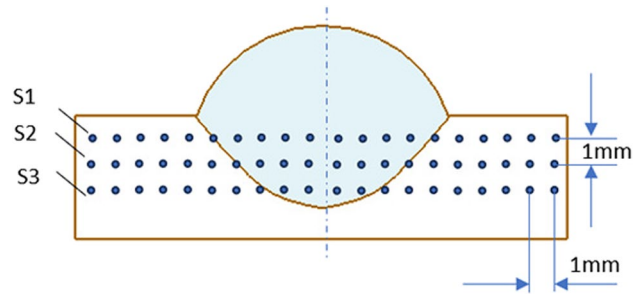


Fig. 6 The distribution of the hardness measurement points

Table 3 The average of hardness in different zones

Sample	AF type	Hardness in WM (HV5)	Hardness in HAZ (HV5)	Hardness in BM (HV5)
1	SiO ₂	413	163.5	161
2	TiO ₂	424	163	165
3	Without AF	330	167	160
4	CaCO ₃	413.4	160	161

separately, which were 13.45 mm and 11.15 mm. The weld reinforcement is also considered for further research as the results showed that the sample with CaCO₃ as the AF can reach a greater bead height. Therefore, CaCO₃ could be considered to improve the manufacturing speed.

3.2 Hardness analysis

3.2.1 Average hardness

The hardness HV5 was tested in straight parallel lines (S1, S2, and S3) as shown in Fig. 6. According to the different hardnesses, three zones are classified: Weld Metal (WM), Heat Affected Zone (HAZ), and Base Metal (BM). The variation in the hardness for the samples welded with and without AF is shown in Table 3 and Fig. 7.

The data revealed that the average hardness of BM is about 160–165 HV5 and the hardness of HAZ is 160–167 HV5. The hardness is significantly different between the samples welded with and without AF for the WM areas. As shown in Table 3, the hardness with AF is 413–424 HV5, while the hardness without AF is only 330 HV5, 29% lower than the highest hardness of 424 HV5 from TiO₂ as AF.

3.2.2 Influence of AF on HAZ

The hardness in BM and WM both has a relatively stable value, while in HAZ, the hardness is constantly changing. Thus, the HAZ region can be obtained through the hardness distribution.

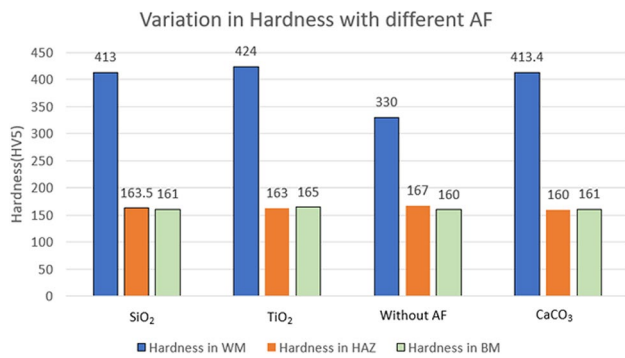


Fig. 7 Variation in hardness with and without fluxes

Figure 8 displays the hardness distribution trends in different welding zones. According to the results, the width of the HAZ for samples welded with AF is wider than for samples welded without AF. Therefore, using AF in GMAW can increase the HAZ width. It is also revealed that the hardness at the BM is maintained at about 160–165, but when it enters the HAZ there is a slight decrease in hardness. The hardness decrease area was named HAZ hardness soften [26], which was caused the temperature impact. When approaching the WM, the hardness gradually increases and finally maintains a certain level in the weld area, which is the hardness of the weldments.

Based on the test results, the width of HAZ (including the grain growth and grain refiner parts) can be evaluated, and the results showed that the width of the HAZ with AF

welded is about 6 mm, while the width of HAZ without AF is about 5 mm.

3.2.3 Influence of AF on WM

The hardness in WM is different between welding samples with and without AF. As mentioned, the hardness without AF welding is around 330 HV, while the other three samples are all above 400 HV, so the effect of AF on hardness is significant. In Fig. 8c, the bottom two lines are straight even in the center and the value is about 160 HV5 like the BM hardness, which means that the penetration is very low for this welding sample in comparison with the sample welded with AF.

3.3 Microstructures

To observe the microstructures of different parts of the welding, two kinds of etchants will be applied for BM/HAZ and WM separately as shown below.

3.3.1 Microstructure of BM and HAZ

In this section, the comparison of the sample using CaCO₃ as AF and without AF was carried out to find out if the AF can influence the BM and HAZ. Hence, 4 vol.% nitric acid-alcohol solution was applied as the etchant to etch the polishing samples, as shown in Fig. 9. The results show that

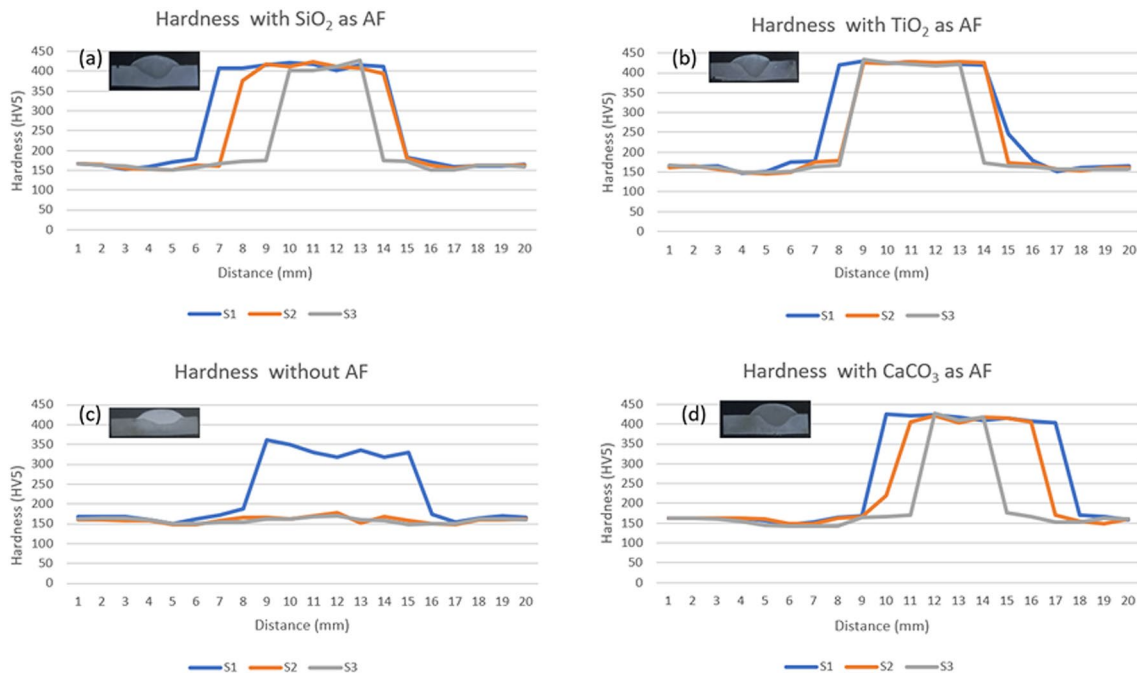
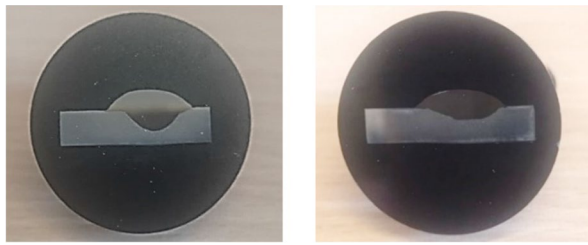


Fig. 8 Hardness distribution trends with and without AF



(a) Welding sample using CaCO_3 as AF (b) welding sample without AF

Fig. 9 Samples after etching with the nitric acid-alcohol solution

only the BM and HAZ were revealed, and the WM was not affected by this solution.

The microstructures of the two samples were observed with a microscope (Nikon Eclipse MA 100). As expected, there are no differences in the BM areas since the grains in the base metal are small and even, as shown in Fig. 10a, b.

The grain size comparison for the boundary of WM and HAZ, in Fig. 10c, f, revealed that the grain size with CaCO_3 is slightly bigger than without AF. Therefore, it can be concluded that AF has little effect on the microstructure of HAZ and BM.

3.3.2 Microstructure of WM

As mentioned in Sect. 2, the Kalling No. 2 reagent was applied for the WM etching, and the microstructure of each sample, which is shown in Fig. 11. Figure 11a, e shows the WM microstructure without AF and revealed that the main structure is even columnar and cellular austenite. With the addition of the AF, the microstructure of WM changed

significantly, as shown in Fig. 11c–h. The more columnar dendritic structure possibly appeared because of higher heat input with the addition of AF. As per Fig. 11c, e, g, it can be observed that there are dark-colored structures on the light-colored austenite matrix, and some lamellar martensite appear. The enlarged view in Fig. 11e, f, h shows the different microstructures in the WM, including ferrite, austenite, and martensite. The presence of martensite may explain the increase in weld hardness with AF.

As shown above, martensite is obtained, which affects the mechanical properties (hardness) of the weldment. Martensite formation can be explained mainly due to the carbon migration from the base metal side into the fusion zone during the welding process. Additionally, the hardness increased much higher than when using the same material, no matter stainless steel, or carbon steel [27, 28].

3.4 Effects of heat treatment on hardness and microstructures

3.4.1 Effects of heat treatment for hardness in WM

The above analysis indicated that the hardness of the weld beads is higher when using AF, so the heat treatments (HT) are considered in this section and the influence of HT with different AF will be discussed in the following.

As mentioned, an annealing temperature of 600 °C and 60 min of annealing time with air cooling was applied. The results showed that there are no significant changes in the BM and HAZ area, so the hardness of WM before and after the HT for each sample is collected and shown in Table 4 and Fig. 12.

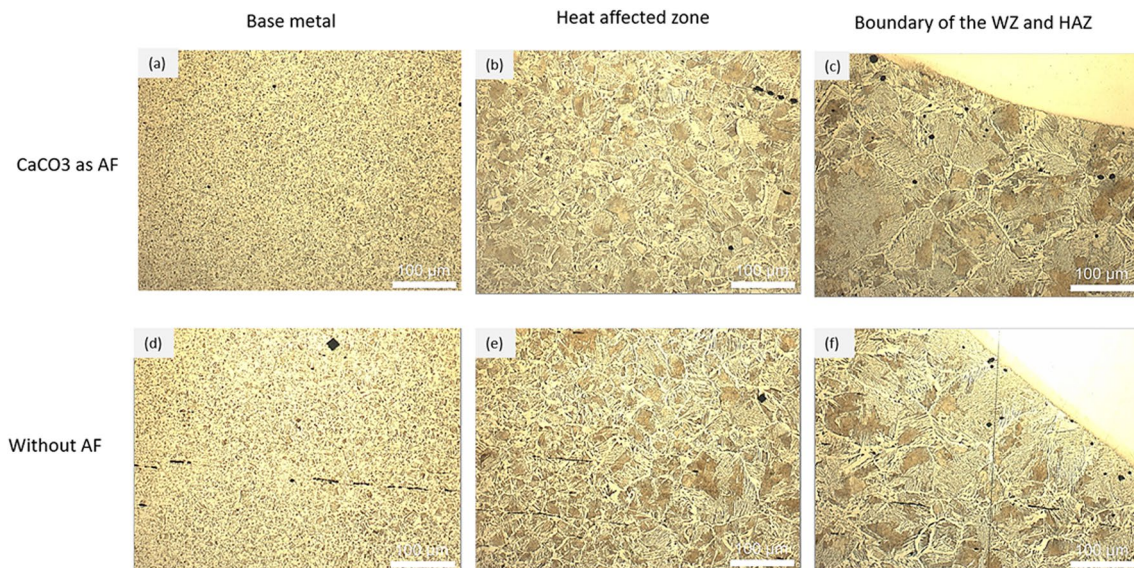
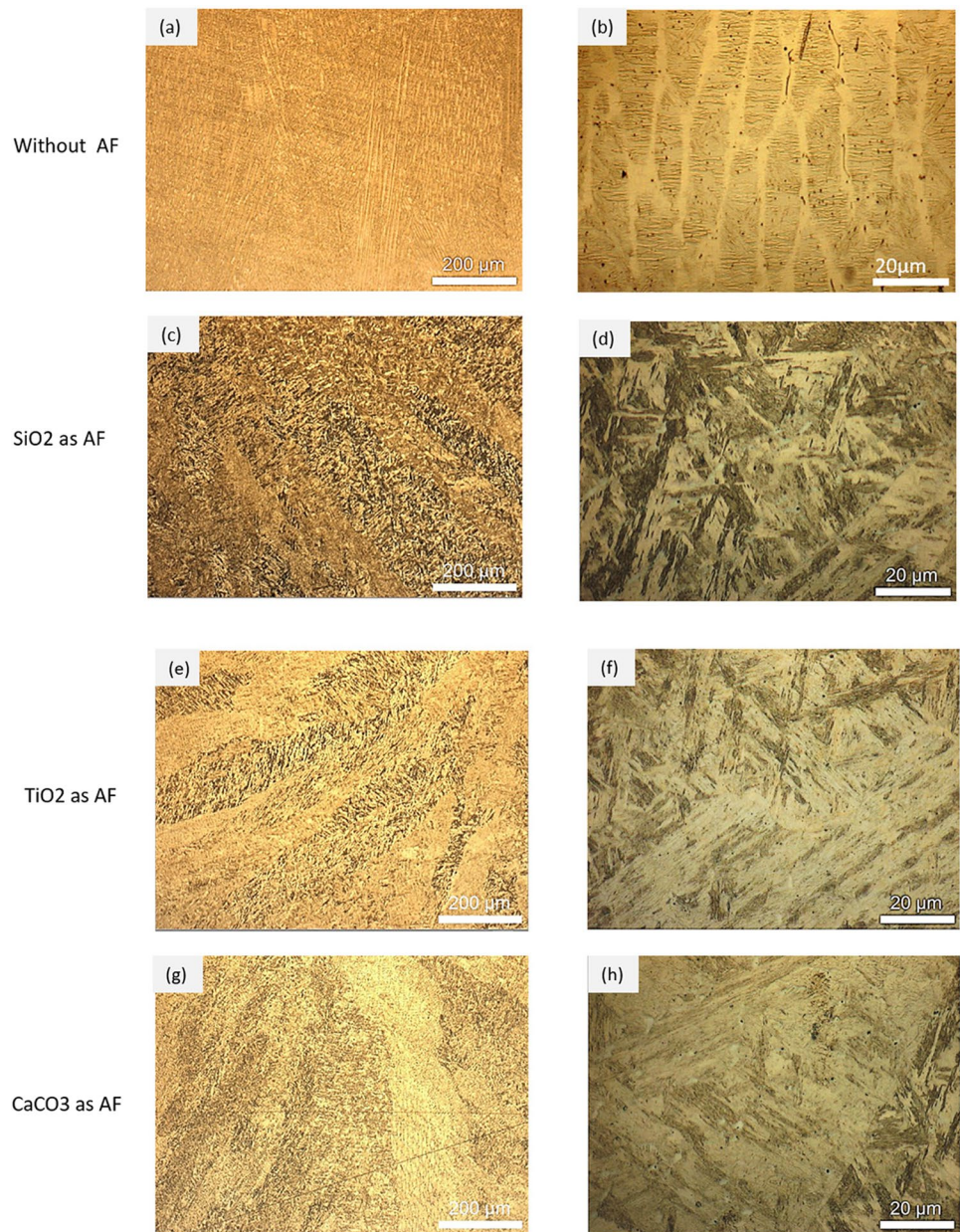


Fig. 10 Microstructure for BM and HAZ

Fig. 11 The microstructures for WM with and without AF



Experiment results indicate that heat treatment has a different effect on welds welded with AF, while there was no reduction of hardness for the sample welded without AF. After the HT, the hardness was similar for all samples. Two reasons could lead to the reduction of hardness. First, at 600 °C, high-temperature heat treatment can release internal stress in the weld and further affect the hardness [29, 30]. At the same time, the martensite in the weld bead undergoes a tempering process, transforming into tempered martensite or other softer phases (such as ferrite).

Table 4 Hardness for WM before and after HT

Samples	AF type	Hardness before HT (HV5)	Hardness after HT (HV5)
1	SiO ₂	413	362
2	TiO ₂	424	359
3	Without AF	330	329
4	CaCO ₃	413.4	348

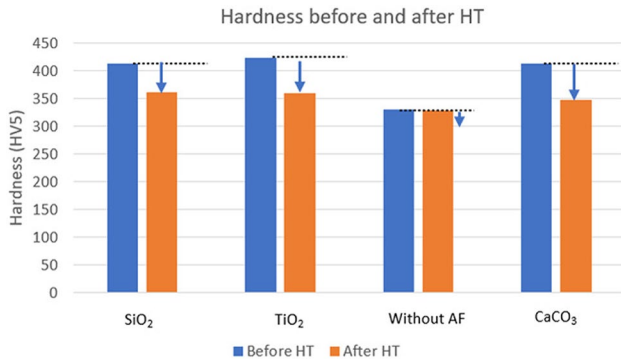


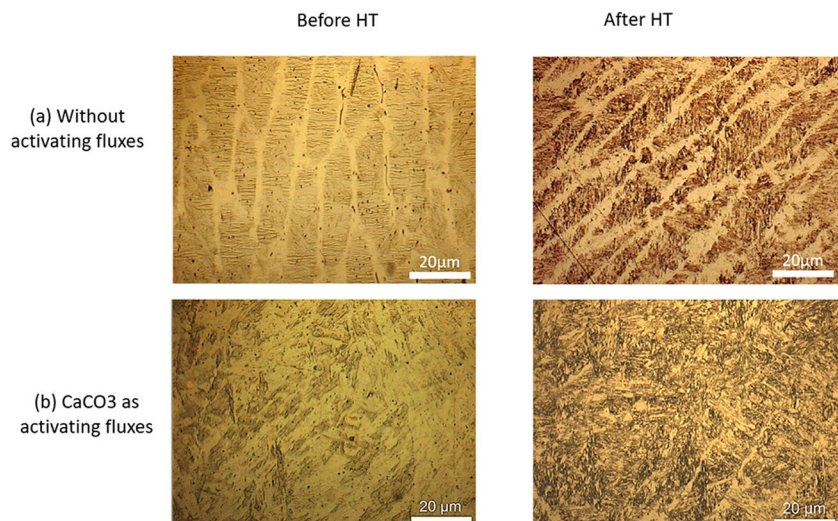
Fig. 12 Hardness before and after HT for WM

3.4.2 Effects of HT on microstructures

The hardness analysis data showed that the hardness at BM and HAZ did not change much, so the study of the microstructure changes will be concentrated in the WM region. Considering that the largest change in hardness was obtained for the sample welded with CaCO₃, the microstructure analysis of the samples without AF and with CaCO₃ as AF was carried out and compared in this section. Figure 13a shows that the microstructure of samples welded without AF changed little after HT.

However, the microstructure obtained by using CaCO₃ as the AF in Fig. 13b presents changes. A comparison of the two figures shows that the structure after HT is more uniform, and large needle-shaped or lath-shaped tempered martensite matrix can be seen with some fine carbide particle distribution.

Fig. 13 Microstructure for WM (S3 and S4) after HT



4 Conclusions

To analyze the influence of AF on geometry and hardness in GMAW, three AF were applied during the 316 L/mild steel welding process, and the conclusions are shown below.

1. AF can improve penetrations in the GMAW process, and the highest penetration (3.85 mm) was obtained using TiO₂ as AF.
2. Reinforcements can also be influenced by AF, and the largest reinforcement (3.47 mm) was obtained when applying CaCO₃ as AF.
3. AF can reduce the weld bead width, and the application of TiO₂ resulted in the smallest width (11.15 mm).
4. There was a significant increase in the hardness of WM when using AF, and TiO₂ obtained the largest average hardness (424HV), which was about 29% higher than the hardness obtained without AF.
5. Microstructures of HAZ and BM showed that there is no significant difference between welds with and without AF.
6. Different microstructures are observed for welds with and without AF for the WM area. Martensite contributed to higher hardness in this area for welds with AF.
7. HT can reduce the hardness significantly for the with AF welding bead, while it contributed little for the without AF.
8. HT improved the microstructures for welds with AF and the grain distribution became more even after the HT.

These studies on the effects of AF on weld morphology and mechanical properties can be served as the basis for subsequent additive manufacturing research, ensuring the dimensional accuracy and mechanical properties of GMAW

additive manufacturing parts while possibly saving energy and improving productivity.

Author contribution Huifeng Wang (PhD student) contributed to the conceptualization of the study, conducted the experiments, collected and analyzed the data, and drafted the initial version of the manuscript. Stefanija Klaric (supervisor) supervised Huifeng Wang throughout the experiment process and critically reviewed and edited the manuscript for intellectual content, clarity, and coherence. Both authors have read and approved the final version of the manuscript.

Declarations

Competing interests The authors declare no competing interests.

References

1. A. Kaloshkar SBM (2022) Activated flux welding: a review. *Int Res J Eng Technol (IRJET)* 09(07):6
2. Huang HY (2010) Effects of activating flux on the welded joint characteristics in gas metal arc welding. *Mater Des* 31(5):2488–2495
3. Baghel A et al (2021) Influence of activated flux on micro-structural and mechanical properties of AISI 1018 during MIG welding. *Mater Today-Proc* 47:6947–6952
4. Chaudhari PG, Patel PB, Patel JD (2018) Evaluation of MIG welding process parameter using activated Flux on SS316L by AHP-MOORA method. *Mater Today-Proc* 5(2):5208–5220
5. Dinaharan I et al (2022) Effect of activating flux on penetration and microstructure of tungsten inert gas-welded pure titanium grade-2 plate. *Int J Adv Manuf Technol* 121(5–6):3399–3417
6. Gao XG, Dong JH, Han X (2017) Effect of RE₂O₃(RE = La, Ce) fluxes on A-TIG welding of Ti6Al4V. *Int J Adv Manuf Technol* 91(1–4):1181–1188
7. Muthukumaran N et al (2022) Comparative studies on weldability and mechanical characteristics of semi-killed steel using different arc welding technique. *Mater Today-Proc* 62:5471–5476
8. Patel NP et al (2021) Review on the use of activated flux in arc and beam welding processes. *Mater Today-Proc* 43:916–920
9. Mei LF et al (2017) Effect of activating flux on laser penetration welding performance of galvanized steel. *Int J Adv Manuf Technol* 91(1–4):1069–1078
10. Vasantharaja P, Vasudevan M, Palanichamy P (2015) Effect of welding processes on the residual stress and distortion in type 316LN stainless steel weld joints. *J Manuf Process* 19:187–193
11. Weng HJ et al (2022) Multi-objective optimizations of the Q355C steel gas metal arc welding process based on the grey correlation analysis. *Int J Adv Manuf Technol* 121(5–6):3567–3582
12. Yue SQ et al (2023) Improving welding penetration and mechanical properties via activated-flux smearing by tungsten inert gas arc welding. *Metals* 13(12)
13. Patel K, Kahar SD (2023) Effect of SiO and TiO flux on metallurgical and corrosion properties of the activated tig welded AA7004 aluminum alloy. *Russ J Non-Ferrous Metals* 64(1–3):1–8
14. Sivateja P, Vidyarthi RS (2024) Influential behavior study of fluxes during activated flux tungsten inert gas welding of IRSM 41 steel. *J Mater Eng Perform.* <https://doi.org/10.1007/s11665-024-09178-z>
15. Abhishek Chakraborty CS (2021) Sandeep Rathee, Manu Srivastava, Influence of activated flux on weld bead hardness of MIG welded austenitic stainless steel. *Mater Today: Proc* 47:6884–6889
16. Balázs Varbai RK (2017) Kornél Májlínger, Effects of active fluxes in gas metal arc welding. *Periodica Polytechnica Mech Eng* 61(1):68–73
17. Ruan Y et al (2012) Mechanical properties and microstructures of 6082–T6 joint welded by twin wire metal inert gas arc welding with the SiO₂ flux. *Mater Des* 35:20–24
18. Bradeesh Moorthy S, M.S., Mohamed Akbaral I (2020) Investigation on the effect of activated flux on metal inert gas weldment. *Int J Eng Res Technol* 9(02):488–491
19. Rosas CHM, Modenesi PJ, Ortiz MR (2020) Effects of active flux on GMAW welding applied to a steel AISI/SAE 1020. *Soldagem Inspecao* 25. <https://doi.org/10.1590/0104-9224/si25.02>
20. Huang YS et al (2024) Effect of PWHT on microstructure and mechanical properties of welded joint of a new Fe-Ni-based superalloy. *Mater Sci Eng a-Struct Mater Prop Microstruct Process* 906
21. Figueiredo GGD et al (2023) Parametric study and response optimization for the wire plus arc additive manufacturing of 316LSi via pulsed GMAW. *Int J Adv Manuf Technol* 129(7–8):3073–3092
22. Xu SH, Wang YD (2015) Estimating the effects of corrosion pits on the fatigue life of steel plate based on the 3D profile. *Int J Fatigue* 72:27–41
23. Wu W et al (2019) Forming process, microstructure, and mechanical properties of thin-walled 316L stainless steel using speed-cold-welding additive manufacturing. *Metals* 9(1):109
24. Khan M, Dewan MW, Sarkar Z (2021) Effects of welding technique, filler metal and post-weld heat treatment on stainless steel and mild steel dissimilar welding joint. *J Manuf Process* 64:1307–1321
25. Jorge JCF et al (2019) Influence of welding procedure and PWHT on HSLA steel weld metals. *J Mater Res Technol-Jmr&T* 8(1):561–571
26. Khan MS et al (2023) A review on heat affected zone softening of dual-phase steels during laser welding. *J Manuf Process* 102:663–684
27. Nayee SG, Badheka VJ (2014) Effect of oxide-based fluxes on mechanical and metallurgical properties of dissimilar activating flux assisted-tungsten inert gas welds. *J Manuf Process* 16(1):137–143
28. Scutelnicu E et al (2021) Metallurgical and mechanical characterization of low carbon steel-stainless steel dissimilar joints made by laser autogenous welding. *Metals* 11(5)
29. Baumgartner J, Bruder T (2013) Influence of weld geometry and residual stresses on the fatigue strength of longitudinal stiffeners. *Welding in the World* 57(6):841–855
30. Kim YK et al (2018) Effect of stress relieving heat treatment on the microstructure and high-temperature compressive deformation behavior of Ti-6Al-4V alloy manufactured by selective laser melting. *Metall Mater Trans-Phys Metall Mater Sci* 49a(11):5763–5774

Publisher's Note Springer Nature remains neutral with regard to jurisdictional claims in published maps and institutional affiliations.

Springer Nature or its licensor (e.g. a society or other partner) holds exclusive rights to this article under a publishing agreement with the author(s) or other rightsholder(s); author self-archiving of the accepted manuscript version of this article is solely governed by the terms of such publishing agreement and applicable law.